TISSUE ENGINEERING: Part A
Volume 21, Numbers 9 and 10, 2015

DOI: 10.1089/ten.tea.2014.0314

Compaction, Fusion, and Functional Activation of Three-Dimensional Human Mesenchymal Stem Cell Aggregate

Ang-Chen Tsai, BS, Yijun Liu, MS, Xuegang Yuan, MS, and Teng Ma, PhD

Human mesenchymal stem cells (hMSCs) are primary candidates in cell therapy and tissue engineering and are being tested in clinical trials for a wide range of diseases. Originally isolated and expanded as plastic adherent cells, hMSCs have intriguing properties of *in vitro* self-assembly into three-dimensional (3D) aggregates that improve a range of biological properties, including multilineage potential, secretion of therapeutic factors, and resistance against ischemic condition. While cell–cell contacts and cell–extracellular matrix interactions mediate 3D cell aggregation, the adaptive changes of hMSC cytoskeleton during self-assembly and associated metabolic reconfiguration may also influence aggregate properties and functional activation. In this study, we investigated the role of actin in regulating 3D hMSC aggregate compaction, fusion, spreading and functional activation. Individual hMSC aggregates with controlled initial cell number were formed by seeding a known number of hMSCs (500, 2000, and 5000 cells/well) in multi-well plates of an ultra-low adherent surface to form multicellular aggregates in individual wells. To assess the influence of actin-mediated contractility on hMSC aggregation and properties, actin modulators, including cytochalasin D (cytoD), nocodazole, lysophosphatidic acid (LPA), and Y-27632, were added at different stages of aggregation and their impacts on hMSC aggregate compaction and apoptosis were monitored. The results suggest that actin-mediated contractility influences hMSC aggregation, compaction, fusion, and spreading on adherent surface. Formation of multi-cellular aggregates significantly upregulated caspase 3/7 expression, expression of C-X-C chemokine receptor type 4 (CXCR-4), cell migration, secretion of prostaglandin E2 (PGE-2) and interleukin 6 (IL-6), and resistance to *in vitro* ischemic stress. The functional enhancement, however, is dependent on caspase activation, because treatment with Q-VD-OPh, a pan-caspase inhibitor, attenuated CXCR-4 and cytokine secretion. Importantly, comparable ATP/cell levels and significantly reduced mitochondrial membrane potential in aggregates of different sizes suggest that altered mitochondria bioenergetics on 3D aggregation is the primary inducer for apoptosis. Together, the results suggest multicellular aggregation as an effective and nongenetic strategy for hMSC functional activation.

Introduction

Human mesenchymal stem cells (hMSCs) are primary candidates in cell therapy and tissue engineering and are being tested in clinical trials for a wide range of diseases. Originally isolated and expanded as plastic adherent cells, culture-expanded hMSCs have been used in diverse diseases based on their capacity for multi-lineage differentiation and secretion of trophic factors that have immune modulatory, anti-inflammatory, and pro-angiogenic properties.[1,2] However, recent studies have shown that hMSC culture expansion on planar adherent surfaces leads to gradual loss of their therapeutic potency with altered immune modulatory properties, low survival rate post-transplantation, and changes in their secretory profile and therapeutic potential due to an increasing senescent subset.[3–5] While the mechanism of the culture-induced changes remains to be determined, factors in the artificial culture environment such as oxidative stress in ambient oxygen condition and rigidity of culture substrate are considered contributing factors to cellular senescence and culture heterogeneity.[2,4,6,7] Thus, strategies that preserve the therapeutic potency of the culture-expanded hMSC are important in translating hMSC to clinical applications.

Human MSCs have intriguing properties of self-assembly into three-dimensional (3D) aggregates that improve a range of biological properties, including multi-lineage potential, expression of migratory cytokine receptor such as C-X-C

Department of Chemical and Biomedical Engineering, Florida State University, Tallahassee, Florida.

chemokine receptor type 4 (CXCR-4), secretion of trophic factors, and resistance against ischemic condition.[8–11] In particular, hMSC aggregation significantly upregulates secretion of anti-inflammatory cytokines via a caspase-dependent mechanism.[11–13] Assembly of multicellular aggregates creates spatial gradients of soluble factors such as oxygen, nutrients, and regulatory macromolecules, and that formation of a hypoxic microenvironment in the interior of the aggregates has been suggested as a potential mechanism for upregulating secretion of pro-angiogenic factors (e.g., VEGF, FGF-F, HGF, and CXCR-4) and extracellular matrix expression.[14,15] Apart from the spatial variation of exogenous and endogenous biochemical molecules, cell aggregation also involves sequential steps of cell detachment, cell–cell contacts, cadherin accumulation, aggregation, and compaction, which drastically changes cell morphology and cytoskeleton arrangement.[16–19] In these processes, the actin-mediated contractility is a dominant force that regulates the mechanical structure of individual cells and re-establishes the balance in tension between the interior compressed cytoskeleton elements such as microtubules and microfilaments and opposing elements such as contractile actin cytoskeleton.[20] To date, the influence of actin-mediated contractility on hMSC morphology and biological properties has been chiefly studied on planar surface[21,22] and its role in regulating 3D aggregate properties and functional activation remains to be elucidated.

According to the differential adhesion hypothesis (DAH), cells have liquid-like properties and can be sorted out from one another based on the strengths of intercellular adhesions expressed as tissue surface tension.[23] After establishment of initial cell–cell contact and adhesion during aggregation, actomyosin-mediated contractility leads to mechanical polarization and upregulation of cortical tension along the external boundary and/or downregulation along internal surfaces.[24] Subsequently, cortical tension at the boundary of the multicellular aggregates dominates the mechanical energy of adhesive bounds, exerting a net mechanical effect on the cells equivalent to extra adhesion among all the cells in the multicellular aggregates. For example, the MSC aggregates undergo considerable compaction and a reduction in diameter of hMSC aggregates from 632 to 353 μm over 21 days has been reported.[25] The spatial differences in the biomechanical environment have also been correlated with alteration in hMSC phenotype and properties such as osteogenic differentiation and secretion of angiogenic factors.[26,27] However, whether actin-mediated aggregate compaction regulates hMSCs functional enhancement remains unknown. There is an increasing interest in applying hMSCs for ischemic cerebral and cardiac vascular diseases, in which cell size, migratory properties, and resistance to ischemic stress are crucial to minimize emboli and increase lifespan of transplanted cells.[28,29] On the other hand, the aggregate biomechanical properties such as compaction and fusion are important in tissue engineering by bio-printing using multi-cellular spheroids as ''bio-ink.''[30] In this study, we investigated the actin-mediated contractility in regulating hMSC 3D aggregation, compaction, fusion, and transition from liquid to solid state. Results also showed that the stress response and associated metabolic alternation instead of actin-mediated compaction are the primary factor for the enhanced cytokine secretion and resistance to *in vitro* ischemic stress.

Materials and Methods

Culture of hMSCs

Frozen hMSCs at passage 1 in liquid nitrogen were obtained from the Tulane Center for Stem Cell Research and Regenerative Medicine. The hMSCs were isolated from the bone marrow of healthy donors ranging in age from 19 to 49 years based on plastic adherence, being negative for CD34, CD45, and CD117 (all < 2%) and positive for CD29, CD44, CD49c, CD90, CD105, and CD147 markers (all > 95%), and possessing tri-lineage differentiation potential on induction *in vitro*.[31] The hMSCs were expanded with minimum essential medium-alpha (Life Technologies, Carlsbad, CA) supplemented with 1% penicillin/streptomycin (Life Technologies) and 10% fetal bovine serum (FBS; Atlanta Biologicals, Lawrenceville, GA) on 150-mm tissue culture Petri dishes (Corning, Corning, NY) at a density of ~1500 cells/cm^2 in a standard 5% CO_2 incubator. The culture media were changed every 3 days. hMSCs from three different donors at passage 5 to 7 were used in the experiments. All reagents were purchased from Sigma-Aldrich (St. Louis, MO) unless otherwise noted.

Aggregate formation and treatment with cytoskeleton modulators

hMSCs from monolayer culture were trypsinized, and 100 μL media containing 5000 cells were added in each well of an ultra-low attachment (ULA) 96-well plate with a round bottom (Corning) overnight. To analyze size-dependent ATP contents, aggregates containing 500, 2000, and 5000 cells were used following the same method. Suspended single hMSCs spontaneously self-assembled into one aggregate per well. Aggregates were cultured individually till 7 days with media changed every 2 days. The aggregates were tracked individually, and the morphologies were imaged with an Olympus IX70 microscope (Center Valley, PA).

Cytochalasin D (cytoD), lysophosphatidic acid (LPA), Y-27632, and nocodazole were added into culture media to final concentrations of 0.2 to 0.6, 2.0 to 10.0, 2.0 to 10 μM, and 1.0 M, respectively. To test the temporal effects of actin modulators on aggregate formation, cells were treated with media containing cytoD and LPA during monolayer culture before aggregate formation (termed ''2D Pretreatment'') or 12 h after aggregate formation in ULA plates (termed ''3D Treatment''). Only 3D treatments were performed for Y-27632 and nocodazole.

Analysis of aggregate size, DNA content, fusion, and spreading on adherent surface

Morphology of the aggregates was visualized using an Olympus IX70 microscope, and the images were recorded. The images were processed, and the areas of the individual aggregates were calculated using ImageJ software (http://rsb.info.nih.gov/ij/). The DNA content of the individual aggregates was used to calculate cell number. Briefly, individually collected hMSC aggregates were washed with phosphate-buffered saline (PBS) and digested with proteinase K overnight. PicoGreen (Life Technologies) was added to triplicate samples and a DNA standard in a 96-well plate. The cell numbers in aggregates were determined by the PicoGreen fluorescence intensity using 9.3 pg/cell as

determined in our previous study.[32] DNA assay detects double-stranded DNA that may also be present in dead cells with intact DNA. However, this population in the aggregates is low, and the yield of live cells measured by DNA assay is close to cell count using other methods such as flow cytometry.[33] The packing densities were calculated using cell number divided by aggregate volume assuming a spherical shape. At least six aggregates were used in each condition.

To test re-adhesion and fusion, the aggregates from various treatment conditions were plated on a glass coverslip for re-adhesion or placed adjacently on ULA surface for fusion. Images were captured with an Olympus IX70 microscope and analyzed by ImageJ software.

Measurement of Caspase 3/7, interleukin 6, and prostaglandin E2

Caspase 3/7 activity was measured by Caspase-Glo 3/7 assay systems (Promega, Madison, WI). Caspase-Glo 3/7 working buffer was added to triplicate samples containing aggregates and culture media in a 96-well LUMITRAC 200 white immunology plate (Greiner Bio-One, Monroe, NC). The results were read by a luminescence plate reader and normalized to cell number (Biotek Instruments, Winooski, VT). Secreted prostaglandin E2 (PGE-2) and interleukin 6 (IL-6) in conditioned media were quantified using a PGE-2 Parameter Assay Kit and IL-6 DuoSet ELISA kits, respectively (R&D Systems, Minneapolis, MN). Total secreted PGE-2 and IL-6 were determined by subtracting cytokine concentrations in culture media controls and normalized to the cell number in the aggregates.

Osteogenic induction, scanning electron microscopy, immunohistochemistry, and histology

After aggregate formation in the ULA culture dishes, the growth media were replaced with osteogenic media (high-glucose Dulbecco's modified Eagle's medium [Life Technologies] supplemented with 10% FBS, 1% penicillin/streptomycin, 100 nM dexamethasone, 10 nM sodium-b-glycerophosphate, and 12.8-mg/L ascorbic acid-2 phosphate) following the previously reported method.[32] After 7 days of incubation, the osteogenic differentiation (OD) induced aggregates were transferred to a glass coverslip for adhesion or were placed adjacently on a ULA surface for fusion.

For scanning electron microscopy (SEM), the aggregate samples were fixed in 4% paraformaldehyde (PFA), dehydrated through a graded series of ethanol, incubated in hexamethyldisilazane, and vacuum dried overnight. The samples were mounted onto carbon-coated chucks, sputter coated with gold in an argon atmosphere for 4 min at 2 kV, and analyzed on an SEM (JSM-7401F; JEOL, Tokyo, Japan). For immunostaining, the cells were fixed with 4% PFA, permeabilized with 0.5% Triton X-100, blocked with 1.0% bovine serum albumin, incubated with primary antibody, and imaged with an Olympus IX70 microscope. For histology, hematoxylin-eosin staining was performed following the previously reported method.[32] hMSC aggregates were fixed in 10% formalin, dehydrated, and embedded in paraffin wax; 10 μm sections were cut and stained with Lerner-2 Hematoxylin (Lerner Laboratories, Pittsburgh, PA) and Eosin-Y w/ Phloxine (Richard-Allan Scientific, Kalamazoo, MI) by standard procedures.[32] Images were captured with an Olympus IX70 microscope with MagnaFire SP 2.1B software.

Flowcytometry, transwell migration assays, and in vitro *ischemia*

Aggregates were dissociated in trypsin, washed in PBS, and fixed at 4% PFA at room temperature. Aliquots of a 100 μL cell suspension were incubated with fluorochrome-conjugated, anti-mouse monoclonal antibody CXCR-4 (R&D Systems). For mitochondrial membrane potential measurement, trypsinized MSCs were washed by centrifugation in warm Hank's balanced salt solution (HBSS). Cell suspension was incubated with tetramethylrhodamine, methyl ester (TMRM; Life Technologies), washed with HBSS, and analyzed by flow cytometry (BD Biosciences, San Jose, CA). Labeled samples were washed in PBS followed by flow cytometry analysis with the isotype controls run in parallel at the same concentration used for each antibody.

A transwell migration system (Neuro Probe, Gaithersburg, MD) was used to study the migration of aggregate-dissociated hMSCs and monolayer-cultured hMSCs in response to human recombinant stromal cell-derived factor 1 (SDF-1) (R&D Systems). A cell migration assay kit using an 8-μM pore size was used. Resuspended cells in serum-free medium were loaded in the top chamber of the migration well. Serum-free medium containing 30 ng/mL of SDF-1 was added to the lower chamber. Cells were incubated at 37°C in 5% CO_2 for 4 h. The remaining cells in the top chamber were scratched, and the migrated cells were stained with Hoechst and counted.

To mimic ischemic conditions, hMSCs dissociated from the aggregates and adherent controls were incubated in serum-free growth media at 1% O_2, controlled in a C-Chamber (BioSpherix, Lacona, NY) for 6 h, and analyzed by Live/Dead staining (Life Technologies). The combination of serum withdrawal and low oxygen tension is known to induce hMSC apoptosis and has been used *in vitro* to mimic ischemic condition.[34]

Statistics

Unless otherwise noted, all experiments were performed at least in triplicate ($n = 3$), and representative data were reported. Experimental results were expressed as means ± standard deviation of the samples. Statistical comparisons were performed by one-way ANOVA and Tukey's *post hoc* test for multiple comparisons, and significance was accepted at $p < 0.05$.

Results

Actin-mediated contractility influences the assembly of multicellular hMSC aggregates

While the initial steps of aggregation require close contact and cell–cell adhesion via cadherin molecules, reorganization of actin cortical network is crucial in the establishment of a mature cell–cell contact.[24] To investigate the temporal effects of actin-mediated contractility in hMSC aggregate formation, hMSC cultures were treated with cytoD (i) in plastic culture for 2 days before cell detachment (e.g., two-dimensional [2D] pretreatment) or (ii) 12 h after aggregate formation on ULA surfaces (i.e., 3D treatment). In 2D pretreatment, hMSC displayed a dose-dependent response in which cytoD disrupted hMSC aggregation at a concentration above 0.6 μM and prevented aggregate compaction at lower concentrations (Fig. 1A, B). In 3D treatment, hMSC aggregates remained

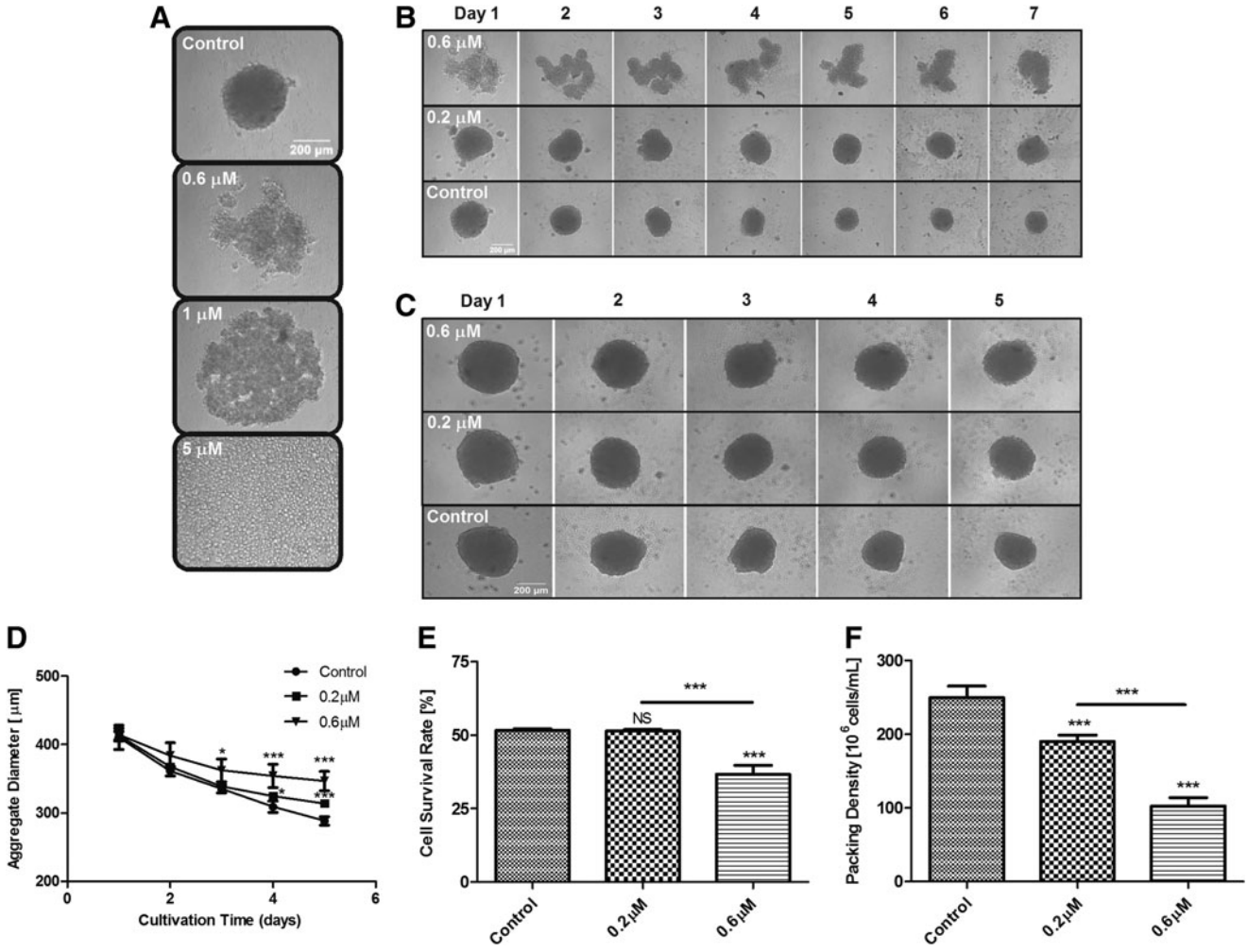

FIG. 1. Cytochalasin D (CytoD) interrupts human mesenchymal stem cell (hMSC) aggregation. **(A)** CytoD treatment prevented hMSC aggregation at high concentration. CytoD treatment reduced compaction of hMSC aggregates at low concentration, and there is no significant difference in compaction between **(B)** two-dimensional (2D)-pretreated and **(C)** three-dimensional (3D)-treated aggregates. **(D)** Dose-dependent decline of aggregate diameters after 3D treatment. However, 0.6 μM cytoD 3D treatment significantly reduced cell viability **(E)** and packing density **(F)** compared with control aggregates at day 5. $*p < 0.05$; $***p < 0.005$; NS, no statistical significance.

intact in cytoD concentration of 0.6 μM and exhibited dose-dependent reduction on compaction similar to those of 2D pretreatment group (Fig. 1B–D). In contrast, cytoD treatment prevented aggregate compaction but reduced cell viability, leading to significantly lower cell survival and packing density compared with control hMSC group at day 5 (Fig. 1E, F).

To investigate the role of microtubule in hMSC aggregates, the hMSC aggregates were treated by nocodazole, a chemical agent that interferes with the polymerization of microtubules. Despite the drastic changes of cell morphology on 2D surface, nocodozole-treated hMSC aggregates have comparable or higher compaction compared with the nontreated controls, suggesting the microtubule is not the major force during aggregate compaction (Fig. 2).

Actin mediates aggregate compaction but not viability and caspase expression

LPA is a naturally occurring bioactive phospholipid with multiple biological functions that include its ability to initiate cytoskeleton contraction by RhoA activation, promote cell survival and proliferation, and enhance survival of hypoxia-challenged neonatal cardiomyocytes.[35,36] LPA has also been identified as a novel survival factor, and it protects MSCs against hypoxia and serum deprivation-induced apoptosis.[37] Treatment of hMSC aggregates by LPA, however, has limited effects on aggregate compaction as well as on viability at LPA concentration till 10 μM (Fig. 3).

The involvement of actin-myosin based contractility was investigated by treatment of aggregates with Y-27632, which inhibits the phosphorylation of Rho-associated kinase (ROCK) and prevents cell compaction.[38] As expected, inhibition of ROCK by 10 μM Y-27632 reduced aggregate compaction with a 6.7% increase in diameter by day 5 and a 38.7% decrease in cell packing density compared with the control aggregates (Fig. 4). Despite significant reduction in aggregate compaction, cell viabilities in the Y-27632-treated aggregates were comparable or even less than those of control aggregates, suggesting reduced compaction by Y-27632 treatment failing to rescue hMSCs in the aggregates.

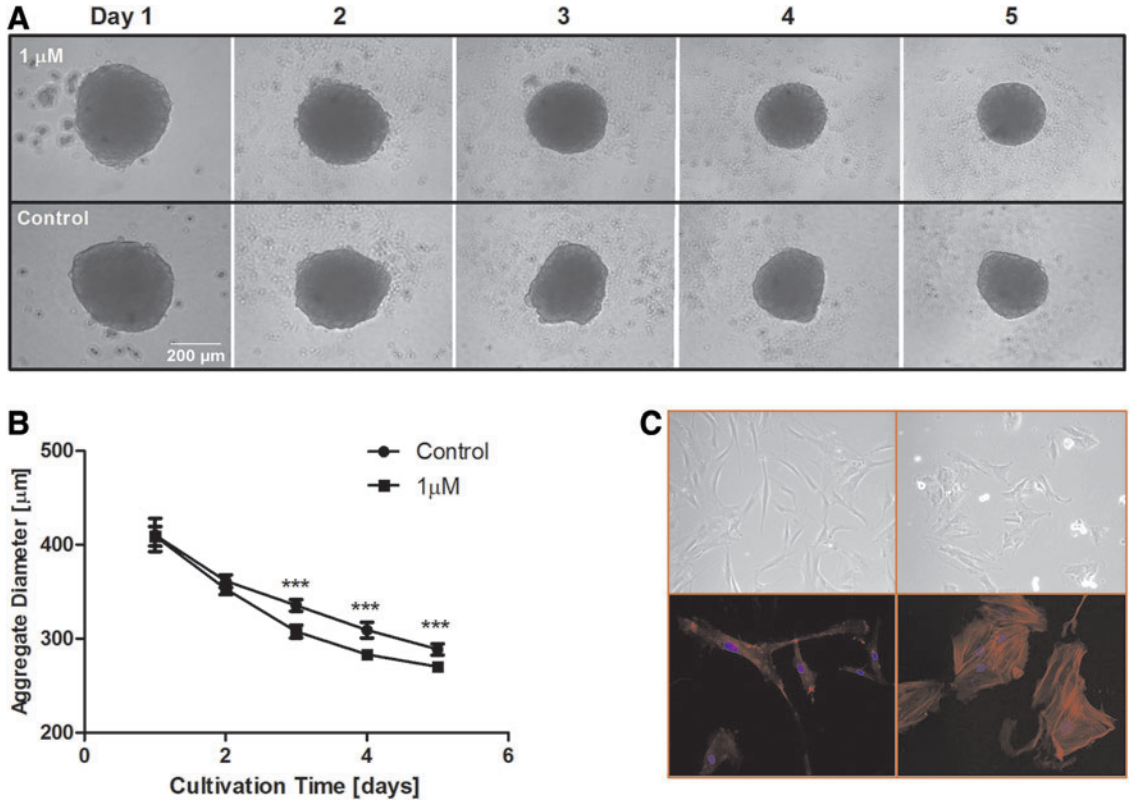

FIG. 2. Aggregate treatment by nocodazole. **(A, B)** Nocodazole-treated hMSC aggregates underwent faster compaction than the control aggregates. **(C)** F-actin structure was stained with phalloidin rhodamine (*red*) and nuclei counterstained with DAPI (*blue*). Nocodazole treatment significantly altered hMSC morphology on planar surface. ***$p < 0.005$. Color images available online at www.liebertpub.com/tea

Previous studies have reported increased apoptosis in hMSC aggregates,[12,13] but the origin of the stress signals remains to be resolved. Measurement of caspase 3/7 activity was used to quantify protein markers involved in late-stage apoptosis owing to its capacity to discriminate between apoptotic and necrotic cells.[39] Compared with their counterparts in adherent 2D culture, formation of multi-cellular aggregates significantly increased caspase 3/7 activity for all treatment groups with the Y-27632-treated aggregates having the highest caspase 3/7 activity. CytoD treatment significantly increased caspase 3/7 activity in 2D adherent culture, whereas cytoD-treated aggregates had comparable apoptotic activity as hMSC control aggregates. Treatment by Y-27632 and LPA also increased caspase 3/7 activity in both 2D culture and 3D aggregates. These results suggest that prevention of aggregate compaction by actin modulators did not significantly reduce apoptosis, although the cytotoxic effects of the actin modulators may be a contributing factor (Fig. 5A).

To determine the relationship between apoptosis and aggregate compaction, hMSC aggregates were treated with Q-VD-OPh, a pan caspase inhibitor. After 3 days of culture, Q-VD-OPh-treated aggregates have reduced compaction and significantly increased cell viability compared with the control, resulting in higher packing density (Fig. 5B–D). These results suggest that cellular apoptosis is upstream of and partially contributes to aggregate compaction.

Actin mediates aggregate morphology, interaction, and spreading on adherent surfaces

Disruption of actin significantly alters hMSC morphology in the aggregates. As shown in Figure 6, cells in the hMSC aggregates were tightly packed and spread with limited interstitial space at the boundary of the aggregate. In contrast, cells in the cytoD- and Y-27632-treated aggregates were loosely packed and exhibited a spherical morphology with abundant interstitial space as shown by SEM and histology (Fig. 6A, A′). Histological sectioning also revealed contrasting morphology of hMSC in the interior of control and cytoD and Y-27632-treated aggregates. In the control aggregates, hMSCs are morphologically heterogeneous with spindle-shaped cells at the outer boundary and round and tightly packed cells in the interior, indicating morphological polarization. In the cytoD and Y-27632-treated aggregates, cells are loosely packed with no spreading at the boundary, indicating the absence of a mechanically polarized outer boundary (Fig. 6B, C).

The tendency of cellular aggregates to spontaneously form spherical aggregates has been suggested to be analogous to the behavior of liquid drops that spontaneously acquire a spherical shape in suspension and fuse when placed in close contact to minimize surface tension.[40] When placed in close contact, untreated hMSC aggregates readily fused and spread on a glass coverslip, so did the ones treated by LPA and

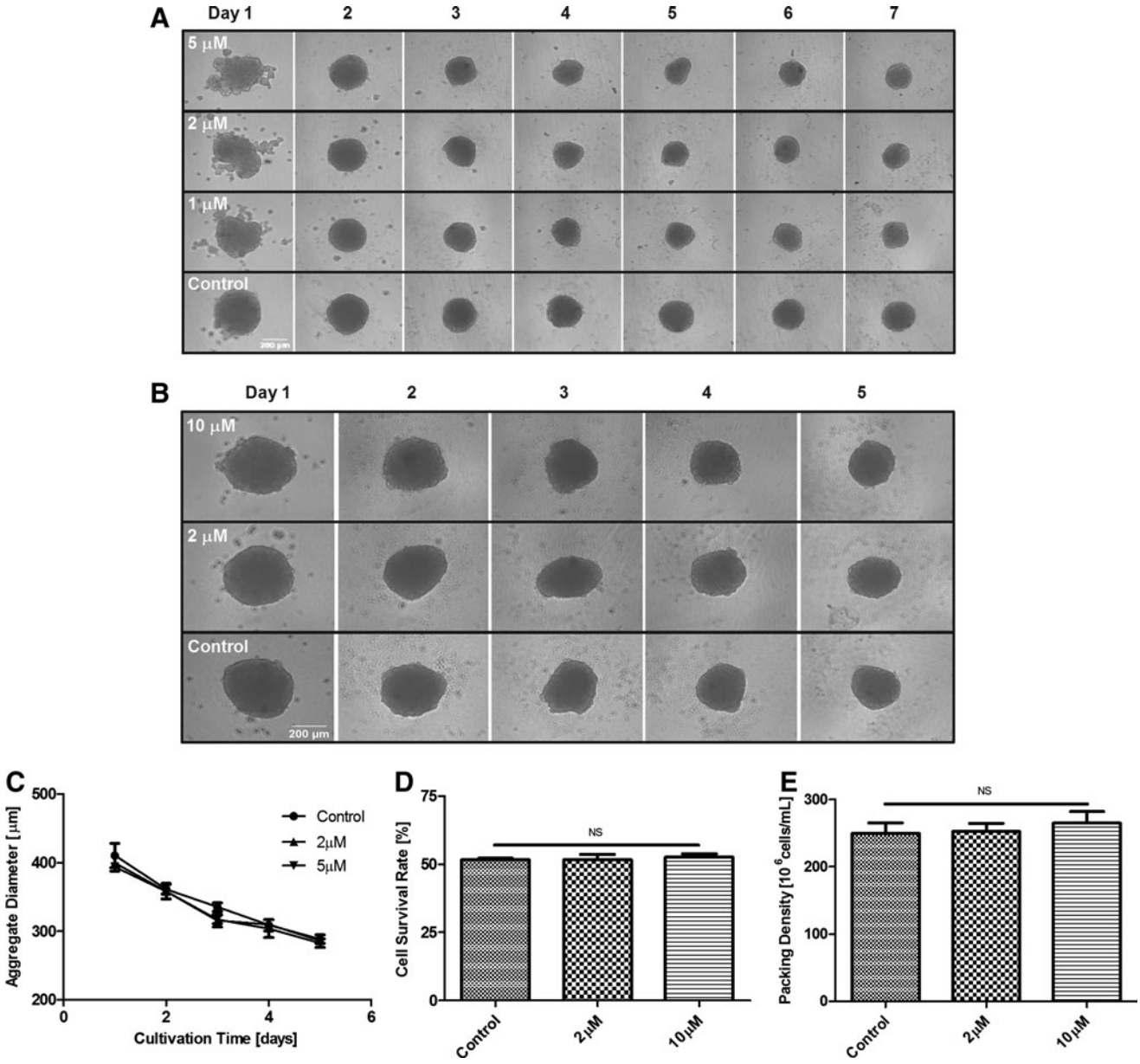

FIG. 3. Lysophosphatidic acid (LPA) treatment has limited effects on hMSC aggregate survival and compaction. Both **(A)** 2D pretreatment and **(B)** 3D treatment by LPA have minimal impact on aggregate compaction. **(C)** Projected areas of the LPA-treated aggregates declined at the same rate as control. After 5 days of LPA 3D treatment, the LPA-treated aggregates have comparable cell survival **(D)** as well as **(E)** cell packing density as the control. NS, no statistical significance.

nocodazole (Fig. 7). Y-27632-treated aggregates spread on glass coverslips but have a reduced tendency to fuse. However, interrupting actin filaments by cytoD completely prevented aggregate spreading on a glass coverslip and fusion of adjacent aggregates. Interestingly, after osteogenic induction, hMSC-OD aggregates maintained their spherical shape on a rigid glass coverslip and failed to fuse when in close contact. These results suggest that the viscoelastic behavior of hMSC aggregates is primarily mediated by actin.

Functional enhancement and metabolic alteration

Formation of 3D multicellular aggregates has been suggested as an important means to precondition hMSCs to enhance their anti-inflammatory properties and therapeutic potency in ischemic cerebral and cardiovascular diseases.[11,41] To evaluate the effects of 3D aggregation on hMSC properties, hMSC dissociated from the aggregates were characterized. As shown in Figure 8, aggregate-derived hMSCs are significantly smaller than the 2D control with a 36% reduction in diameter in suspension (Fig. 8A, B). After replating the aggregate-derived hMSCs on plastic culture dishes, they are also significantly smaller than their 2D counterparts (Fig. 8C). Aggregate-derived hMSCs also have significantly higher CXCR-4 expression and stronger migration ability toward SDF-1, as indicated by transwell migration assay (Fig. 8D, E). To further characterize hMSC's resistance to ischemic stress, aggregate-derived hMSCs and control from 2D

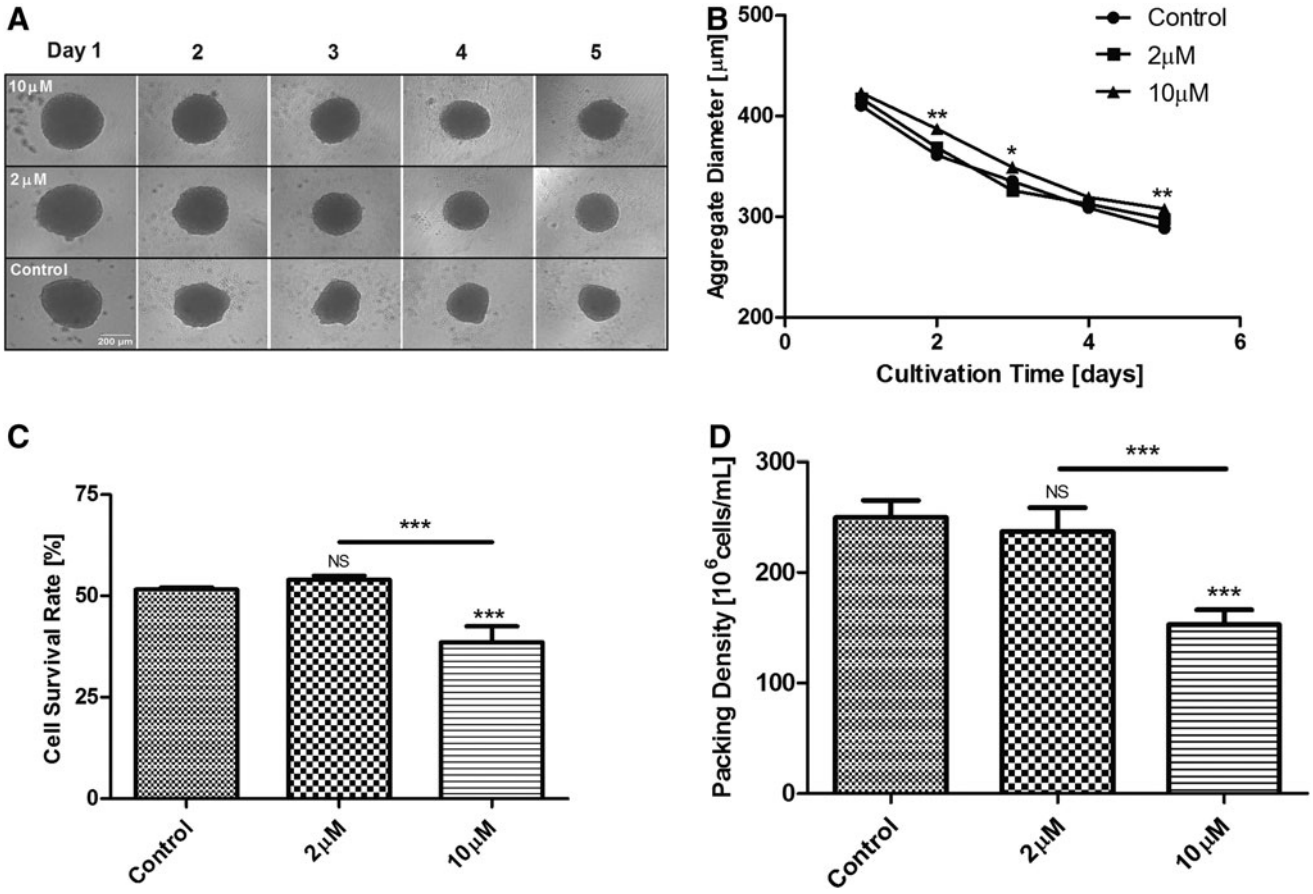

FIG. 4. Aggregate treatment by Rho-associated kinase (Rock) inhibitor Y-27632. Treatment by Y-27632 prevented aggregate compaction **(A)** with reduced decline in diameter of aggregates **(B)**. **(C)** After 5 days of treatment, cell survival in the 10 μM Y-27632-treated aggregates is lower than nontreated control. **(D)** By day 5, cell packing density of Y-27632-treated aggregates is significantly lower compared with the control. *$p < 0.05$; **$p < 0.01$; ***$p < 0.005$; NS, no statistical significance.

adherent cultures were subject to *in vitro* ischemic (i.e., serum-free and 1% O_2) that mimics *in vivo* ischemic condition (Fig. 8F).[34] The results showed that aggregate-derived hMSCs have significantly higher survival under ischemic stress compared with their 2D counterparts. Collectively, the enhanced expression of CXCR-4, migration in response to SDF-1, resistance to ischemic stress, along with reduced cell size suggest the beneficial impact of 3D aggregation on hMSC properties in ischemic injuries.

Elevated secretion of anti-inflammatory cytokine such as IL-6 and PGE-2 is thought to be due to hMSC stress response via caspase-mediated mechanism.[12,41] To investigate whether caspase inhibition attenuates hMSC secretory function, the aggregates were treated with Q-VD-OPh. As shown in Figure 8G and H, formation of 3D aggregates significantly upregulated the secretion of IL-6 and PGE-2 but this enhancement is attenuated to basal levels in the presence of Q-VD-OPh, suggesting the stress-induced functional activation in 3D aggregates. In addition, secretion of IL-6 and PGE-2 is independent from aggregate compaction, because CytoD and Y-27632 treatment has limited effects on the levels of of IL-6 and PGE-2.

To identify the source of stress signal and determine whether the impediment of oxygen and nutrients due to diffusion alters bioenergetics and results in apoptosis, cellular ATP contents/cell in aggregates of different sizes (e.g., 500, 2000, and 5000 cells/aggregates) were measured and compared with the adherent cells. All three aggregates have comparable ATP/cell contents, but all are $< 1/3$ of the adherent cells (Fig. 9A). The aggregate-size independent ATP/cell contents suggest diffusion limitation is not a primary factor for the reduced metabolic activity but aggregation altered hMSC energy metabolism. Indeed, accompanying the reduced ATP content, the aggregates have significantly reduced mitochondrial membrane potential as measured by TMRM staining (Fig. 9B), suggesting increased mitochondrial depolarization as the major contributing factor to cellular apoptosis in 3D aggregates.

Discussion

Actin-mediated contractility influences hMSC aggregation, compaction, and fusion

Isolated partially based on their plastic adherence, hMSCs are highly sensitive to biomechanical cues and substrate elasticity, which regulate hMSC lineage commitment and differentiation by modulating cytoskeletal tension and RhoA activation.[21,42] The tension-mediated signaling is manifested in cytoskeletal contractility, in which reorganization of actin microfilaments plays a major role in hMSC

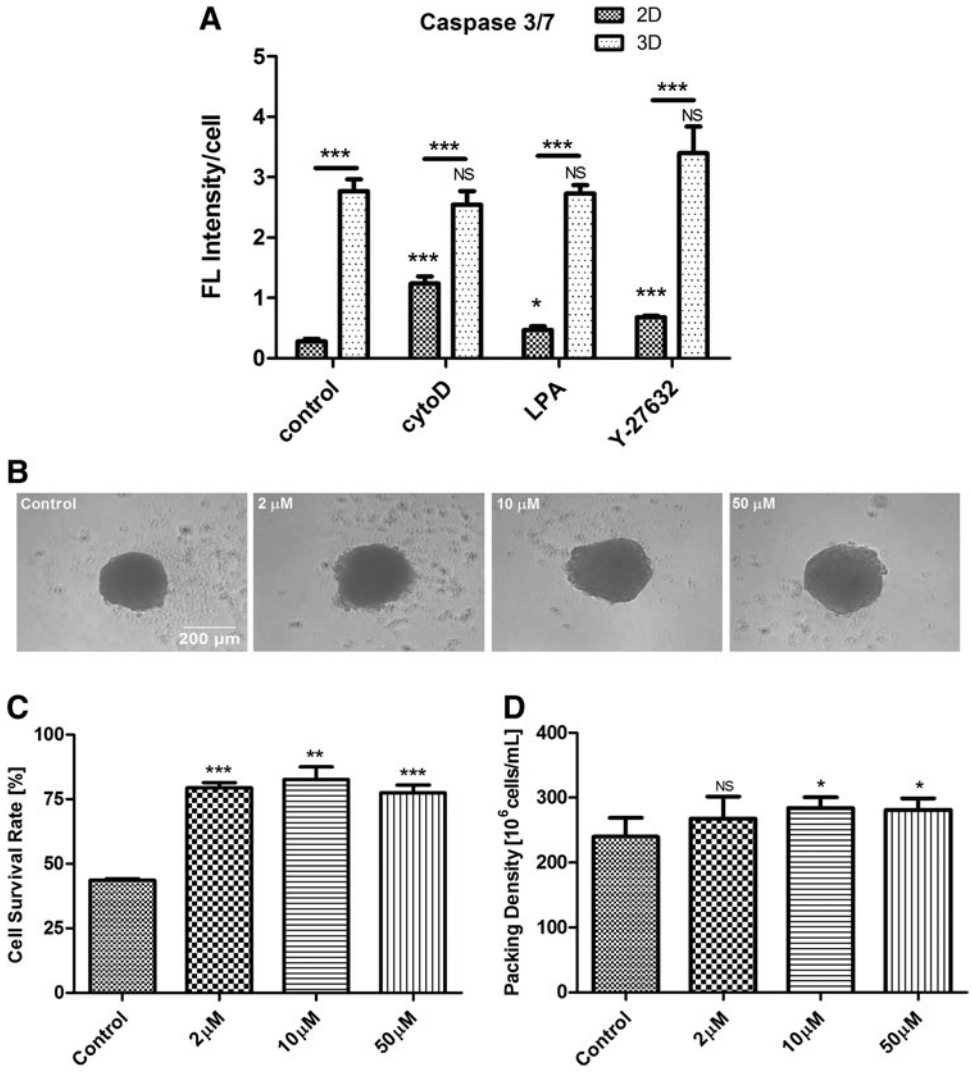

FIG. 5. Caspase expression and inhibition. **(A)** Formation of 3D aggregates significantly increased caspase 3/7 expression compared with 2D adherent culture for all treatment groups. Treatment by pan caspase inhibitor Q-VD-OPh significantly reduced cell compaction **(B)**, improved cell survival **(C)**, and increased cell packing density **(D)**. *$p < 0.05$; **$p < 0.01$; ***$p < 0.005$; NS, no statistical significance.

realignment on topographical features and response to mechanical stimuli.[43,44] However, these studies have focused on the biomechanical cues on planar surfaces with primary impact on cell morphology and spreading.[21] In 3D setting, actin-mediated contractility not only influences cell rounding, cell–cell contacts, and compaction but also leads to biomechanical polarization that is known to play important roles in tissue organization and morphogenesis.[24] While studies have shown that 3D aggregation profoundly influences hMSC biological properties, the role of actin-mediated contractility in mediating the biomechanical properties of 3D aggregates such as fusion and spreading is yet to be fully understood.

Self-assembly of multicellular aggregates involves sequential steps of cell rounding, initial cell–cell contact, cadherin accumulation, and aggregate compaction, and it requires re-establishment of the balance between surface and cortical tensions mediated by actin.[10] According to the DAH by Steinberg,[23,45] cadherins play a fundamental role in cell sorting and aggregation during tissue development and its perturbation interrupts limb development *in vivo* and influences hMSC multi-lineage differentiation *in vitro*.[46–48] However, this physics-based reasoning has been challenged by recent experimental evidence that adhesive molecules at the cortices of adhering cells not only mechanically couple the neighboring cells but also initiate local reorganization of actomyosin machinery that lead to ''mechanical polarization'' of initially identical cells at the boundary of a cell colony or aggregate.[24,49] As a result, surface tension of aggregates is influenced by actomyosin-driven cell cortical contractility in multicellular aggregates.[50,51] Indeed, our results demonstrate that actomyosin contractility plays a crucial role in regulating hMSC aggregation and that disruption of actin filaments or inhibiting the phosphorylation of myosin light chain by Y-27632 prevented aggregate formation and reduced aggregate compaction in a dose-dependent manner.

Actin contractility also plays a major role in mediating aggregate fusion and spreading on a rigid adherent surface in which disruption of actin by cytoD abolishes spreading and fusion of adjacent aggregates. In contrast, hMSC aggregates treated with nocodazole exhibited comparable contractility with control aggregates, readily spread on adherent surface, and fused with neighboring aggregates, confirming actomyosin-mediated contractility as the main force in aggregate compaction, spreading, and fusion. These results are in

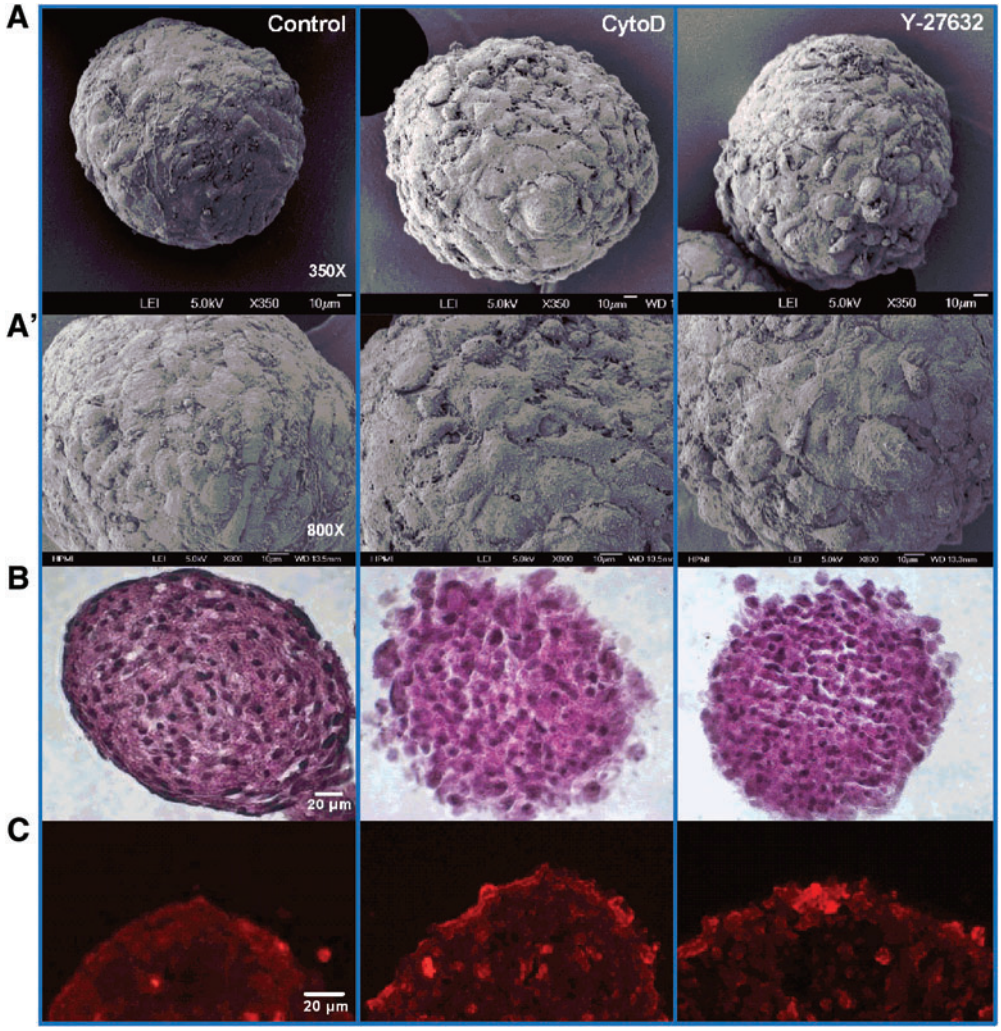

FIG. 6. Morphology of 3D hMSC aggregates. **(A, A′)** Treatment by CytoD and Y-27632 significantly altered cell morphology in the aggregates as shown by scanning electron microscopy images. Cells in the control aggregates spread on an aggregate surface with intimate cell–cell contacts. However, both cytoD- and Y-27632-treated aggregates have large interstitial space and exhibit a round morphology. **(B)** Hematoxylin-eosin staining (pink) of control aggregates showed intact cortical actomyosin outer boundary, whereas disintegrated outer boundaries were observed in the Y-27632- and CytoD-treated aggregates. **(C)** F-actin staining (red) of the histological sections indicated a discontinuous outer boundary for the Y-27632- and CytoD-treated aggregates compared with control aggregate. Color images available online at www.liebertpub.com/tea

agreement with the tensegrity model of cell structure and support the notion that microtubules act as noncompressive structures of cytoskeleton to resist contractile tension of the actin, and its inhibition has limited impact on aggregate compaction.[52] It is of interest to note that the induction of osteogenic differentiation significantly reduced hMSC-OS aggregate spreading on adherent surfaces and fusion with neighboring aggregates. Osteogenic differentiation of hMSCs is accompanied by remarkable changes in cytoskeletal organization from a large number of thin, parallel actin microfilament bundles to a few thick actin filament bundles and corresponding changes in cell biomechanical properties.[53,54] These changes are thought to be induced by osteoinductive components such as dexamethasone, which is known to increase cell stiffness by influencing polymerization of actin microfilaments.[55] Indeed, when placed in close contact, hMSC and OD aggregates displayed markedly different fusion properties with hMSC aggregates spread and enveloped OD aggregates (Supplementary Fig. S1; Supplementary Data are available online at www.liebertpub.com/tea). On the other hand, hMSC aggregates maintained in growth media have comparable fusion properties even after extended culture till 21 days (Supplementary Fig. S2). A recent study suggests that chondrogenic induction by transforming growth factor-beta (TGF-β) leads to hMSC condensation and boundary formation.[56] Together, these results suggest that hMSC phenotypic differentiation determines 3D aggregates' biomechanical properties and influences their self-assembly into functional units through cell fusion and sorting.[10,30]

Caspase-dependent functional activation

Caspase-dependent mechanism has been suggested as a major mechanism in functional activation associated with 3D hMSC aggregation, but the origin of the apoptotic signal remains unclear. Aggregates of undifferentiated hMSCs

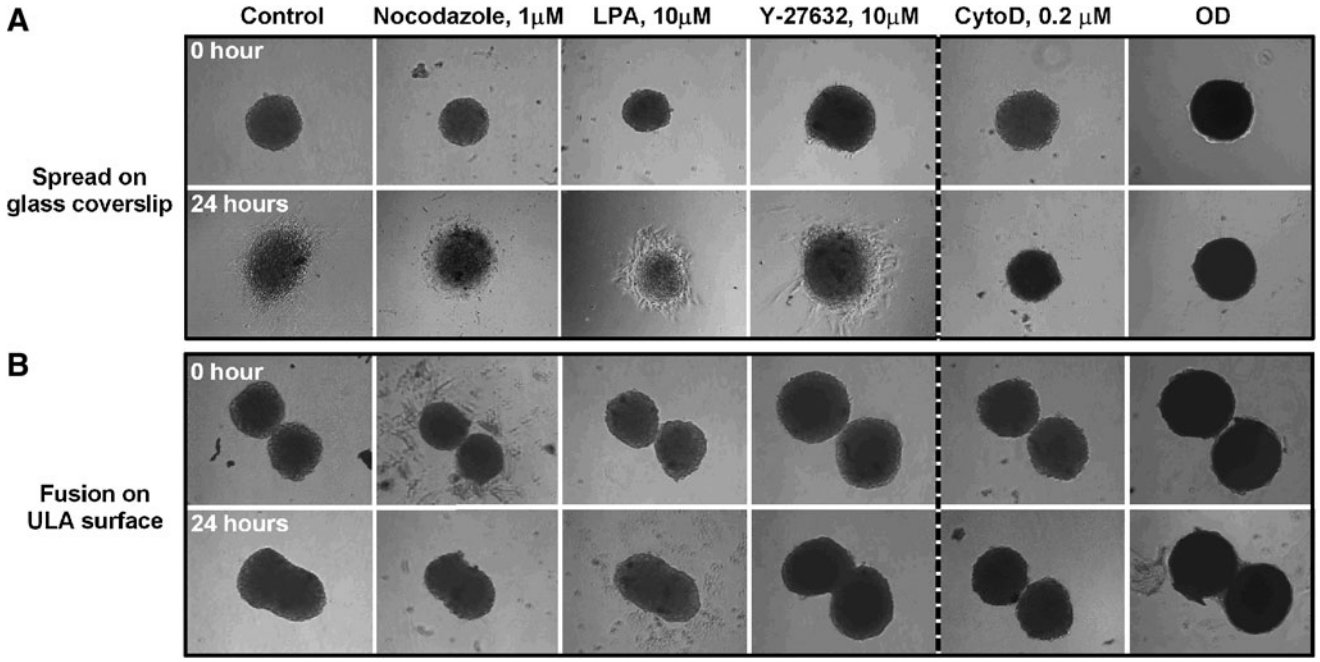

FIG. 7. Aggregate spreading on glass coverslip **(A)** and fusion on ultra-low attachment (ULA) surface **(B)**. Aggregates treated by nocodazole, LPA, and Y-27632 for 5 days readily re-adhered and spread on glass coverslips and fused when adjacently placed on ULA surface. Aggregates treated by cytoD for 5 days or predifferentiated into osteoblasts neither spread on glass coverslips nor fused when placed in close contact. Osteogenic differentiation (OD): hMSC aggregates treated with osteogenic induction medium for 7 days.

experience considerable compaction and a marked decrease in relative amount of cytoplasm and cell volume and an increase in packing density.[12] As such, aggregate compaction has been suggested as a contributing factor to self-activate caspase-dependent signaling and secretion of trophic factors.[12,13] However, reducing aggregate compaction by cytoD and Y-27632 treatments neither led to increased cell viability nor reduced caspase 3/7 expression. While the actin modulators are pleiotropic and have cytotoxic effects on cell viability,[57] their limited reduction on aggregate caspase 3/7 expression in contrast to the significantly increased cell viability by caspase inhibitor (Fig. 5) suggests an independent mediator for caspase activation in 3D aggregates.

Apart from biomechanical forces, impediments of oxygen transport and the resultant hypoxia region in the aggregates have been cited as a cellular stressor for the increase in caspase expression and subsequent functional activation.[8] However, the comparable levels of size-independent ATP/cell in aggregates of different sizes provide direct evidence that oxygen diffusion is not a limiting factor in energy metabolism in the aggregates. In previous studies, immunostaining of the apoptotic activity in 3D hMSC aggregates revealed even distribution of apoptotic cells[13] and that functional enhancement was also observed in aggregates below the threshold of oxygen transport.[11,41] In addition, oxygen is not limiting for electron transport in mitochondria until levels are extremely low; even at an O_2 concentration of 25 μM, electron transport is reduced only by 33%.[58] Thus, oxygen gradient is unlikely a direct contributing factor to the elevated apoptosis.

The comparable ATP/cell levels in aggregates of different sizes and their significant reduction compared with adherent cells suggest that the changes in metabolic machinery after aggregation are independent from diffusion-induced substrate gradients. The drastic changes in cellular organization and creation of a cellular and extracellular microenvironment during multicellular assembly of hMSCs 3D aggregates require effective reconfiguration of a metabolic network for cell survival and function. hMSCs have been shown to use both glycolysis and OXPHO for ATP generation, exhibit metabolic flexibility for survival in an ischemic environment, and undergo coordinated changes of mitochondrial biogenesis during osteogenic differentiation.[59,60] The significant reduction of ATP/cell and the altered mitochondrial potential on aggregation suggest changes in mitochondrial function that may directly contribute to the increased apoptosis. In contrast to mitochondrial transformation that usually occurs during cell differentiation or carcinogenesis, mitochondrial plasticity, known as mitoplasticity, plays an important role in the maintenance of cellular energy homeostasis and influences cell fate in response to energy imbalance due to accidental environmental changes in energy demand or supply.[61] The drastic changes in actin dynamics during 3D aggregation may play a role in the altered mitochondria function in the aggregates as actin cytoskeleton influences mitochondrial organization, short-range movement, and function in mammalian cells.[62,63] One way that actin organization and dynamics in the cell influence mitochondrial network is by changes in the availability of polymerizable actin, thereby influencing morphology, connectivity, and ATP production of the mitochondrial network.[64,65] In addition, the actin cytoskeleton is also an important physiological regulator of reactive oxygen species release from mitochondria and a

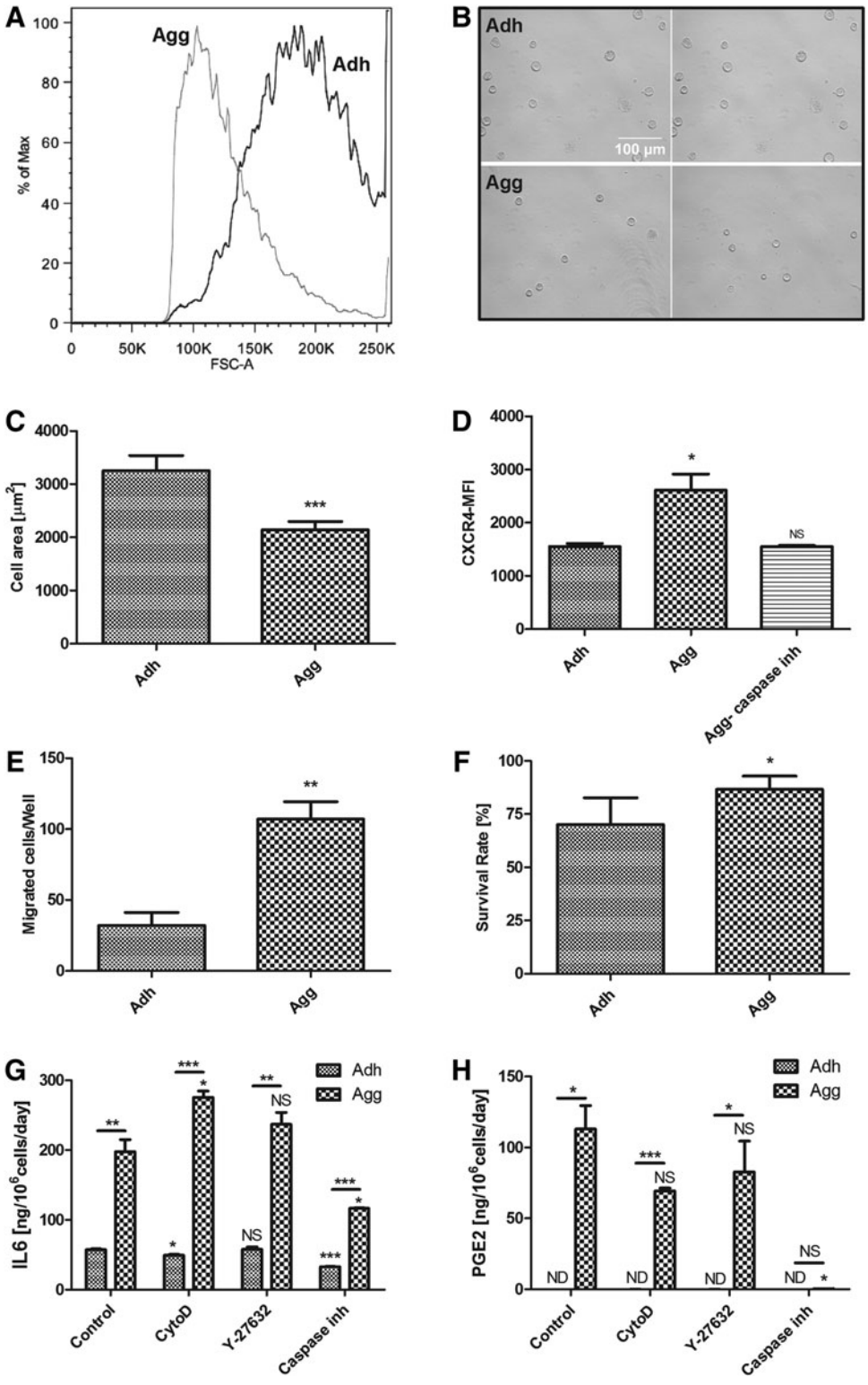

FIG. 8. Cell size, morphology, migration, and hypoxia resistance of aggregate-derived hMSCs. hMSCs dissociated from aggregates are significantly smaller measured by flow cytometry **(A)** and light microscope **(B)** compared with 2D adherent control. When replated and cultured for 24 h, aggregate-dissociated hMSCs are smaller compared with 2D adherent control **(C)**. hMSCs dissociated from aggregates have significantly higher C-X-C chemokine receptor type 4 (CXCR-4) expression measured by mean fluorescent intensity by flow cytometry **(D)** and higher migration toward stromal cell-derived factor 1 (SDF-1), in transwell assay **(E)**. **(F)** hMSCs dissociated from aggregates have higher resistance to *in vitro* ischemia compared with 2D adherent control. hMSC aggregates have significantly higher levels of interleukin 6 (IL-6) **(G)** and prostaglandin E2 (PGE-2) **(H)** expression compared with 2D adherent control, but the elevated expressions were attenuated by Q-VD-OPh, a pan caspase inhibitor to basal levels. CytoD and Y-27632 treatment have limited effects on IL-6 and PGE-2 secretion. $^{*}p < 0.05$; $^{**}p < 0.01$; $^{***}p < 0.005$; NS, no statistical significance; ND, not detectable.

reduction in actin dynamics leads to reduced mitochondria membrane potential, suggesting its key role in the upstream action of apoptosis pathways.[57] Apart from actin, mitochondrial properties in the aggregates may also be influenced and/or mitigated by mitogenic growth factors. Indeed, recent studies have shown that media composition and the presence of mitogenic factors in media significantly influence cell proliferation and secretory functions in the aggregates.[11,33,66] Thus, further studies are warranted to decipher the exact contribution of actin-mediated biomechanical changes and metabolic adaption and apoptosis in hMSC aggregate's functional activation.

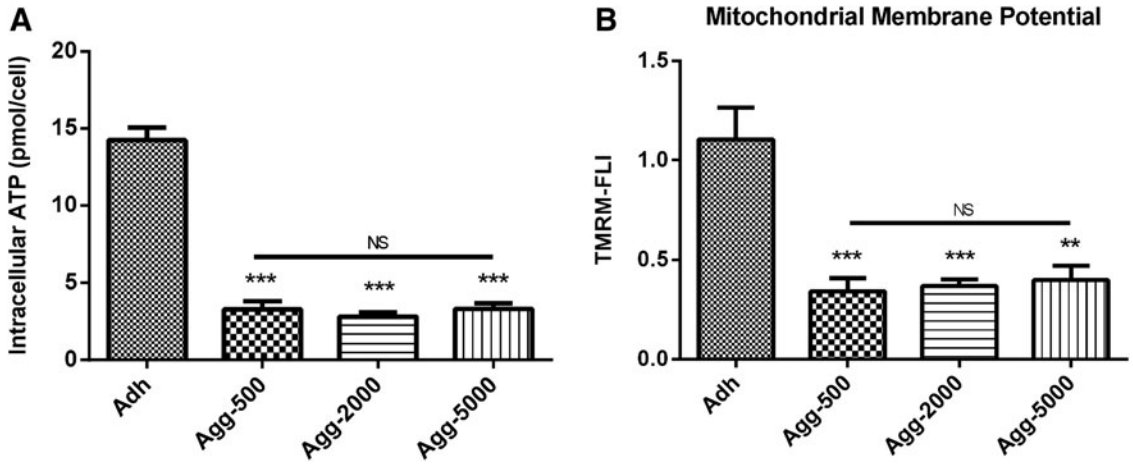

FIG. 9. Intracellular ATP and mitochondrial membrane potential. **(A)** Aggregates of 500, 2000, and 5000 cells/aggregate have comparable levels of intracellular ATP/cell, but all are significantly lower than that of 2D adherent cells. **(B)** Formation of aggregates significantly increased tetramethylrhodamine, methyl ester (TMRM) mean fluorescent intensity, indicating reduced mitochondrial membrane potential. $^{**}p < 0.01$; $^{***}p < 0.005$.

Aggregation as a preconditioning strategy for hMSC functional activation

Spontaneous multicellular aggregation appears to select cells that are small in size, have higher CXCR-4 expression, higher migration, and higher resistance to ischemic stress *in vitro*, suggesting the potential of aggregation as a preconditioning strategy for enhancing hMSC therapeutic properties (Fig. 8). IL-6 is a cytokine that not only is involved in inflammation but also has many regenerative and anti-inflammatory functions,[67] whereas PGE-2 is an important component of hMSC secretome that modulates both innate and adaptive immune responses.[68] Our results confirmed previous observations and demonstrated that the enhanced secretion of IL-6 and PGE-2 is dependent on hMSC stress response and elevated apoptosis activity because the attenuation of apoptosis significantly reduced both PGE-2 and IL-6 secretions.

The results of this study demonstrate that actin-mediated contractility regulates biomechanical properties of aggregates such as compaction, fusion, and spreading, and that 3D aggregation alters mitochondrial properties and induces cellular stress response and functional activation. The results also show that functional activation is regulated by caspase activation during aggregation but is independent from actin-mediated compaction. Further studies are required to determine whether aggregation-mediated cellular events lead to phenotype selection and/or preconditioning at an individual cell level. Previous studies have shown that hMSC *in vitro* aging after extensive passaging altered mitochondrial morphology and decreased antioxidant capacities with reduced actin dynamic and migratory properties.[69,70] Thus, the drastic changes in cytoskeleton during 3D aggregation may select a subset of hMSC that have dynamic actin turnover characteristic of MSC from young donor and enable them to effectively adapt during aggregate compaction. It is also possible that formation of 3D aggregates reverts hMSC to an early phenotype as occurred when neural stem cells formed 3D neurospheres.[71] Nevertheless, the results of this study support that notation that 3D aggregation significantly influences hMSC properties and has the potential as a nongenetic preconditioning method to enhance the function and therapeutic outcome of the culture-expanded hMSC in a wide range of diseases.

Acknowledgment

Funding support from the James King Biomedical Research Program (4KB09 and 3KF05 to T.M.) is acknowledged.

Disclosure Statement

No competing financial interests exist.

References

1. Prockop, D.J., Kota, D.J., Bazhanov, N., and Reger, R.L. Evolving paradigms for repair of tissues by adult stem/progenitor cells (MSCs). J Cell Mol Med **14,** 2190, 2010.
2. Stroncek, D.F., Sabatino, M., Ren, J., England, L., Kuznetsov, S.A., Klein, H.G., and Robey, P.G. Establishing a bone marrow stromal cell transplant program at the national institutes of health clinical center. Tissue Eng Part B Rev **20,** 200, 2014.
3. Bara, J.J., Richards, R.G., Alini, M., and Stoddart, M.J. Bone marrow-derived mesenchymal stem cells change phenotype following *in vitro* culture: Implications for basic research and the clinic. Stem Cells **32,** 1713, 2014.
4. Whitfield, M.J., Lee, W.C.J., and Van Vliet, K.J. Onset of heterogeneity in culture-expanded bone marrow stromal cells. Stem Cell Res **11,** 1365, 2013.
5. Sepulveda, J.C., Tome, M., Fernandez, M.E., Delgado, M., Campisi, J., Bernad, A., and Gonzalez, M.A. Cell senescence abrogates the therapeutic potential of human mesenchymal stem cells in the lethal endotoxemia model. Stem Cells **32,** 1865, 2014.

6. Russell, K.C., Phinney, D.G., Lacey, M.R., Barrilleaux, B.L., Meyertholen, K.E., and O'Connor, K.C. *In vitro* high-capacity assay to quantify the clonal heterogeneity in trilineage potential of mesenchymal stem cells reveals a complex hierarchy of lineage commitment. Stem Cells **28,** 788, 2010.
7. Wagner, W., Horn, P., Castoldi, M., Diehlmann, A., Bork, S., Saffrich, R., Benes, V., Blake, J., Pfister, S., Eckstein, V., and Ho, A.D. Replicative senescence of mesenchymal stem cells: a continuous and organized process. PLoS One **3,** e2213, 2008.
8. Bartosh, T.J., Ylostalo, J.H., Mohammadipoor, A., Bazhanov, N., Coble, K., Claypool, K., Lee, R.H., Choi, H., and Prockop, D.J. Aggregation of human mesenchymal stromal cells (MSCs) into 3D spheroids enhances their antiinflammatory properties. Proc Natl Acad Sci U S A **107,** 13724, 2010.
9. Potapova, I.A., Brink, P.R., Cohen, I.S., and Doronin, S.V. Culturing of human mesenchymal stem cells as three-dimensional aggregates induces functional expression of CXCR4 that regulates adhesion to endothelial cells. J Biol Chem **283,** 13100, 2008.
10. Sart, S., Tsai, A.C., Li, Y., and Ma, T. Three-dimensional aggregates of mesenchymal stem cells: cellular mechanisms, biological properties, and applications. Tissue Eng Part B Rev **20,** 365, 2014.
11. Zimmermann, J.A., and Mcdevitt, T.C. Pre-conditioning mesenchymal stromal cell spheroids for immunomodulatory paracrine factor secretion. Cytotherapy **16,** 331, 2014.
12. Bartosh, T.J., Ylostalo, J.H., Bazhanov, N., Kuhlman, J., and Prockop, D.J. Dynamic compaction of human mesenchymal stem/precursor cells into spheres self-activates caspase-dependent IL1 signaling to enhance secretion of modulators of inflammation and immunity (PGE2, TSG6, and STC1). Stem Cells **31,** 2443, 2013.
13. Kelm, J.M., Breitbach, M., Fischer, G., Odermatt, B., Agarkova, I., Fleischmann, B.K., and Hoerstrup, S.P. 3D microtissue formation of undifferentiated bone marrow mesenchymal stem cells leads to elevated apoptosis. Tissue Eng Part A **18,** 692, 2012.
14. Zhang, Q.Z., Nguyen, A.L., Shi, S.H., Hill, C., Wilder-Smith, P., Krasieva, T.B., and Le, A.D. Three-dimensional spheroid culture of human gingiva-derived mesenchymal stem cells enhances mitigation of chemotherapy-induced oral mucositis. Stem Cells Dev **21,** 937, 2012.
15. Bhang, S.H., Cho, S.W., La, W.G., Lee, T.J., Yang, H.S., Sun, A.Y., Baek, S.H., Rhie, J.W., and Kim, B.S. Angiogenesis in ischemic tissue produced by spheroid grafting of human adipose-derived stromal cells. Biomaterials **32,** 2734, 2011.
16. Lin, R.Z., and Chang, H.Y. Recent advances in three-dimensional multicellular spheroid culture for biomedical research. Biotechnol J **3,** 1172, 2008.
17. Lin, R.Z., Chou, L.F., Chien, C.C.M., and Chang, H.Y. Dynamic analysis of hepatoma spheroid formation: roles of E-cadherin and beta 1-integrin. Cell Tissue Res **324,** 411, 2006.
18. Ivascu, A., and Kubbies, M. Diversity of cell-mediated adhesions in breast cancer spheroids. Int J Oncol **31,** 1403, 2007.
19. Baraniak, P.R., Cooke, M.T., Saeed, R., Kinney, M.A., Fridley, K.M., and McDevitt, T.C. Stiffening of human mesenchymal stem cell spheroid microenvironments induced by incorporation of gelatin microparticles. J Mech Behav Biomed Mater **11,** 63, 2012.
20. Fletcher, D.A., and Mullins, D. Cell mechanics and the cytoskeleton. Nature **463,** 485, 2010.
21. Kilian, K.A., Bugarija, B., Lahn, B.T., and Mrksich, M. Geometric cues for directing the differentiation of mesenchymal stem cells. Proc Natl Acad Sci U S A **107,** 4872, 2010.
22. Dalby, M.J., Gadegaard, N., Tare, R., Andar, A., Riehle, M.O., Herzyk, P., Wilkinson, C.D.W., and Oreffo, R.O.C. The control of human mesenchymal cell differentiation using nanoscale symmetry and disorder. Nat Mater **6,** 997, 2007.
23. Steinberg, M.S. On the mechanism of tissue reconstruction by dissociated cells. I. Population kinetics, differential adhesiveness. and the absence of directed migration. Proc Natl Acad Sci U S A **48,** 1577, 1962.
24. Amack, J.D., and Manning, M.L. Knowing the boundaries: extending the differential adhesion hypothesis in embryonic cell sorting. Science **338,** 212, 2012.
25. Hildebrandt, C., Buth, H., and Thielecke, H. A scaffold-free *in vitro* model for osteogenesis of human mesenchymal stem cells. Tissue Cell **43,** 91, 2011.
26. Rivron, N.C., Vrij, E.J., Rouwkema, J., Le Gac, S., van den Berg, A., Truckenmuller, R.K., and van Blitterswijk, C.A. Tissue deformation spatially modulates VEGF signaling and angiogenesis. Proc Natl Acad Sci U S A **109,** 6886, 2012.
27. Nelson, C.M., Jean, R.P., Tan, J.L., Liu, W.F., Sniadecki, N.J., Spector, A.A., and Chen, C.S. Emergent patterns of growth controlled by multicellular form and mechanics. Proc Natl Acad Sci U S A **102,** 11594, 2005.
28. Toma, C., Wagner, W.R., Bowry, S., Schwartz, A., and Villanueva, F. Fate of culture-expanded mesenchymal stem cells in the microvasculature *in vivo* observations of cell kinetics. Circ Res **104,** 398, 2009.
29. Copland, I.B., and Galipeau, J. Death and inflammation following somatic cell transplantation. Semin Immunopathol **33,** 535, 2011.
30. Jakab, K., Norotte, C., Marga, F., Murphy, K., Vunjak-Novakovic, G., and Forgacs, G. Tissue engineering by self-assembly and bio-printing of living cells. Biofabrication **2,** 022001, 2010.
31. Munoz, N., Kim, J., Liu, Y., Logan, T.M., and Ma, T. Gas chromatography-mass spectrometry analysis of human mesenchymal stem cell metabolism during proliferation and osteogenic differentiation under different oxygen tensions. J Biotechnol **169,** 95, 2014.
32. Kim, J., and Ma, T. Bioreactor strategy in bone tissue engineering: pre-culture and osteogenic differentiation under two flow configurations. Tissue Eng Part A **18,** 2354, 2012.
33. Ylostalo, J.H., Bartosh, T.J., Tiblow, A., and Prockop, D.J. Unique characteristics of human mesenchymal stromal/progenitor cells pre-activated in 3-dimensional cultures under different conditions. Cytotherapy **16,** 1486, 2014.
34. Kim, J., and Ma, T. Endogenous extracellular matrices enhance human mesenchymal stem cell aggregate formation and survival. Biotechnol Prog **29,** 441, 2013.
35. Tigyi, G., Dyer, D.L., and Miledi, R. Lysophosphatidic acid possesses dual-action in cll-proliferation. Proc Natl Acad Sci U S A **91,** 1908, 1994.

36. Moolenaar, W.H. Lysophosphatidic acid, a multifunctional phospholipid messenger. J Biol Chem **270,** 12949, 1995.
37. Chen, J.H., Baydoun, A.R., Xu, R.X., Deng, L.Z., Liu, X.B., Zhu, W.Q., Shi, L.H., Cong, X.F., Hu, S.S., and Chen, X. Lysophosphatidic acid protects mesenchymal stem cells against hypoxia and serum deprivation-induced apoptosis. Stem Cells **26,** 135, 2008.
38. Chen, G.K., Hou, Z.G., Gulbranson, D.R., and Thomson, J.A. Actin-myosin contractility is responsible for the reduced viability of dissociated human embryonic stem cells. Cell Stem Cell **7,** 240, 2010.
39. Elmore, S. Apoptosis: a review of programmed cell death. Toxicol Pathol **35,** 495, 2007.
40. Gonzalez-Rodriguez, D., Guevorkian, K., Douezan, S., and Brochard-Wyart, F. Soft matter models of developing tissues and tumors. Science **338,** 910, 2012.
41. Ylostalo, J.H., Bartosh, T.J., Coble, K., and Prockop, D.J. Human mesenchymal stem/stromal cells cultured as spheroids are self-activated to produce prostaglandin E2 that directs stimulated macrophages into an anti-inflammatory phenotype. Stem Cells **30,** 2283, 2012.
42. McBeath, R., Pirone, D.M., Nelson, C.M., Bhadriraju, K., and Chen, C.S. Cell shape, cytoskeletal tension, and RhoA regulate stem cell lineage commitment. Dev Cell **6,** 483, 2004.
43. Zhao, F., Veldhuis, J.J., Duan, Y.J., Yang, Y., Christoforou, N., Ma, T., and Leong, K.W. Low oxygen tension and synthetic nanogratings improve the uniformity and stemness of human mesenchymal stem cell layer. Mol Ther **18,** 1010, 2010.
44. Engler, A.J., Sen, S., Sweeney, H.L., and Discher, D.E. Matrix elasticity directs stem cell lineage specification. Cell **126,** 677, 2006.
45. Steinberg, M.S. On the mechanism of tissue reconstruction by dissociated cells, III. Free energy relations and the reorganization of fused, heteronomic tissue fragments. Proc Natl Acad Sci U S A **48,** 1769, 1962.
46. Oberlender, S.A., and Tuan, R.S. Expression and functional involvement of N-cadherin in embryonic limb chondrogenesis. Development **120,** 177, 1994.
47. Shin, C.S., Lecanda, F., Sheikh, S., Weitzmann, L., Cheng, S.L., and Civitelli, R. Relative abundance of different cadherins defines differentiation of mesenchymal precursors into osteogenic, myogenic, or adipogenic pathways. J Cell Biochem **78,** 566, 2000.
48. Yeh, H.Y., Liu, B.H., and Hsu, S.H. The calcium-dependent regulation of spheroid formation and cardiomyogenic differentiation for MSCs on chitosan membranes. Biomaterials **33,** 8943, 2012.
49. Maitre, J.L., Berthoumieux, H., Krens, S.F.G., Salbreux, G., Julicher, F., Paluch, E., and Heisenberg, C.P. Adhesion functions in cell sorting by mechanically coupling the cortices of adhering cells. Science **338,** 253, 2012.
50. Krieg, M., Arboleda-Estudillo, Y., Puech, P.H., Kafer, J., Graner, F., Muller, D.J., and Heisenberg, C.P. Tensile forces govern germ-layer organization in zebrafish. Nat Cell Biol **10,** 429, 2008.
51. Manning, M.L., Foty, R.A., Steinberg, M.S., and Schoetz, E.M. Coaction of intercellular adhesion and cortical tension specifies tissue surface tension. Proc Natl Acad Sci U S A **107,** 12517, 2010.
52. Ingber, D.E., and Tensegrity, I. Cell structure and hierarchical systems biology. J Cell Sci **116,** 1157, 2003.
53. Rodriguez, J.P., Gonzalez, M., Rios, S., and Cambiazo, V. Cytoskeletal organization of human mesenchymal stem cells (MSC) changes during their osteogenic differentiation. J Cell Biochem **93,** 721, 2004.
54. Titushkin, I., and Cho, M. Modulation of cellular mechanics during osteogenic differentiation of human mesenchymal stem cells. Biophys J **93,** 3693, 2007.
55. Puig, F., Gavara, N., Sunyer, R., Carreras, A., Farre, R., and Navajas, D. Stiffening and contraction induced by dexamethasone in alveolar epithelial cells. Exp Mech **49,** 47, 2009.
56. Bhumiratana, S., Eton, R.E., Oungoulian, S.R., Wan, L.Q., Ateshian, G.A., and Vunjak-Novakovic, G. Large, stratified, and mechanically functional human cartilage grown *in vitro* by mesenchymal condensation. Proc Natl Acad Sci U S A **111,** 6940, 2014.
57. Gourlay, C.W., and Ayscough, K.R. The actin cytoskeleton: a key regulator of apoptosis and ageing? Nat Rev Mol Cell Biol **6,** 583, 2005.
58. Chandel, N.S., Budinger, G.R., and Schumacker, P.T. Molecular oxygen modulates cytochrome c oxidase function. J Biol Chem **271,** 18672, 1996.
59. Chen, C.T., Shih, Y.R.V., Kuo, T.K., Lee, O.K., and Wei, Y.H. Coordinated changes of mitochondrial biogenesis and antioxidant enzymes during osteogenic differentiation of human mesenchymal stem cells. Stem Cells **26,** 960, 2008.
60. Mylotte, L.A., Duffy, A.M., Murphy, M., O'Brien, T., Samali, A., Barry, F., and Szegezdi, E. Metabolic flexibility permits mesenchymal stem cell survival in an ischemic environment. Stem Cells **26,** 1325, 2008.
61. Jose, C., Melser, S., Benard, G., and Rossignol, R. Mitoplasticity: adaptation biology of the mitochondrion to the cellular redox state in physiology and carcinogenesis. Antioxid Redox Signal **18,** 808, 2013.
62. Sheng, Z.H., and Cai, Q. Mitochondrial transport in neurons: impact on synaptic homeostasis and neurodegeneration. Nat Rev Neurosci **13,** 77, 2012.
63. Quintero, O.A., DiVito, M.M., Adikes, R.C., Kortan, M.B., Case, L.B., Lier, A.J., Panaretos, N.S., Slater, S.Q., Rengarajan, M., Feliu, M., and Cheney, R.E. Human Myo19 is a novel myosin that associates with mitochondria. Curr Biol **19,** 2008, 2009.
64. Yu, Y.S., Dumollard, R., Rossbach, A., Lai, F.A., and Swann, K. Redistribution of mitochondria leads to bursts of ATP production during spontaneous mouse oocyte maturation. J Cell Physiol **224,** 672, 2010.
65. Jayashankar, V., and Rafelski, S.M. Integrating mitochondrial organization and dynamics with cellular architecture. Curr Opin Cell Biol **26,** 34, 2014.
66. Alimperti, S., Lei, P., Wen, Y., Tian, J., Campbell, A.M., and Andreadis, S.T. Serum-free spheroid suspension culture maintains mesenchymal stem cell proliferation and differentiation potential. Biotechnol Prog **30,** 974, 2014.
67. Scheller, J., Chalaris, A., Schmidt-Arras, D., and Rose-John, S. The pro- and anti-inflammatory properties of the cytokine interleukin-6. Biochim Biophys Acta **1813,** 878, 2011.
68. Aggarwal, S., and Pittenger, M.F. Human mesenchymal stem cells modulate allogeneic immune cell responses. Blood **105,** 1815, 2005.
69. Kasper, G., Mao, L., Geissler, S., Draycheva, A., Trippens, J., Kuhnisch, J., Tschirschmann, M., Kaspar, K., Perka, C.,

Duda, G.N., and Klose, J. Insights into mesenchymal stem cell aging: involvement of antioxidant defense and actin cytoskeleton. Stem Cells **27,** 1288, 2009.

70. Geissler, S., Textor, M., Kuhnisch, J., Konnig, D., Klein, O., Ode, A., Pfitzner, T., Adjaye, J., Kasper, G., and Duda, G.N. Functional comparison of chronological and *in vitro* aging: differential role of the cytoskeleton and mitochondria in mesenchymal stromal cells. PLoS One **7,** e52700, 2012.
71. Pastrana, E., Silva-Vargas, V., and Doetsch, F. Eyes wide open: a critical review of sphere-formation as an assay for stem cells. Cell Stem Cell **8,** 486, 2011.

Address correspondence to:
Teng Ma, PhD
Department of Chemical and Biomedical Engineering
Florida State University
2525 Pottsdamer Street
Tallahassee, FL 32310

E-mail: teng@eng.fsu.edu

Received: May 29, 2014
Accepted: February 5, 2015
Online Publication Date: March 18, 2015